



Published in final edited form as:

Cell Res. 2010 June ; 20(6): 665–675. doi:10.1038/cr.2010.40.

BNIP3 is Essential for Mediating 6-thioguanine-and 5-fluorouracil-induced Autophagy Following DNA Mismatch Repair Processing

Xuehuo Zeng^{1,2} and Timothy J. Kinsella^{1,2,*}

¹Department of Radiation Oncology, Case Western Reserve University, Cleveland, OH

²Case Integrative Cancer Biology Program, Case Western Reserve University, Cleveland, OH

Abstract

DNA mismatch repair (MMR) processes the chemically-induced mispairs following treatment with clinically important nucleoside analogs such as 6-thioguanine (6-TG) and 5-fluorouracil (5-FU). MMR processing of these drugs has been implicated in activation of a prolonged G₂/M cell cycle arrest for repair and later induction of apoptosis and/or autophagy for irreparable DNA damage. In this study, we investigated the role of BNIP3 in the activation of autophagy and the temporal relationship between a G₂/M cell cycle arrest and the activation of BNIP3-mediated autophagy following MMR processing of 6-TG and 5-FU. We found that BNIP3 protein levels are up-regulated in a MLH1 (MMR⁺)-dependent manner following 6-TG and 5-FU treatment. Subsequent siRNA-mediated BNIP3 knockdown abrogates 6-TG-induced autophagy. We also found that p53 knockdown or inhibition of mTOR activity by rapamycin cotreatment impairs 6-TG and 5-FU-induced up-regulation of BNIP3 protein levels and autophagy. Furthermore, suppression of Chk1 expression and a subsequent reduction in 6-TG-induced G₂/M cell cycle arrest by Chk1 siRNA promotes the extent of 6-TG-induced autophagy. These findings suggest that BNIP3 mediates 6-TG- and 5-FU induced autophagy in a p53- and mTOR-dependent manner. Additionally, the duration of Chk1-activated G₂/M cell cycle arrest determines the level of autophagy following MMR processing of these nucleoside analogs.

Keywords

BNIP3; p53; mTOR; autophagy; nucleoside analogs

Introduction

DNA mismatch repair (MMR) is one of several DNA repair processes that are vital for maintaining genome stability [1]. It corrects not only mismatches but also insertion-deletion loops (IDLs) which may occur during replication and recombination of DNA. DNA mismatches or IDLs are recognized and initially bound by either MutS α , a heterodimer of

Users may view, print, copy, download and text and data- mine the content in such documents, for the purposes of academic research, subject always to the full Conditions of use: http://www.nature.com/authors/editorial_policies/license.html#terms

*Correspondence to: Timothy J. Kinsella, M.D., Department of Radiation Oncology, Rhode Island Hospital, Physicians Office Building, Suite 130, 110 Lockwood St., Providence, RI 02903, Tel: (401) 444-8402, Fax: (401) 444-7002, timothy.kinsella@case.edu.

MSH2 and MSH6, or MutS β , a heterodimer of MSH2 and MSH3, respectively. Following binding to DNA mispairs or IDLs and undergoing ATP-hydrolysis-dependent conformational transitions, the MutS α or MutS β complexes further recruit another heterodimeric complex of MLH1 and PMS2 (MutL α) to activate subsequent MMR steps such as the excision of the mispairs or IDLs and the resynthesis of the DNA strand [1, 2]. MMR deficiency is associated with human hereditary nonpolyposis colorectal cancer and a modest percentage (up to 15%) of several common sporadic solid tumors, indicating that MMR functions as an important tumor suppression mechanism [3].

MMR also plays an important role in the cytotoxic effects of several classes of clinically active chemotherapy drugs including: methylating agents such as temozolomide; platinum analogs including cisplatin and carboplatin; and nucleoside analogs such as 6-thioguanine (6-TG) and 5-fluorouracil (5-FU) [2, 3]. In response to these DNA damaging agents, MMR has been implicated in initially activating a G₂/M cell cycle arrest followed by the activation of programmed cell death pathways including both apoptosis [2, 3] and autophagy [4, 5].

Since these DNA damaging agents are clinically used in cancer therapy, there is considerable interest in understanding the molecular mechanisms controlling these cellular processes. To this end, 6-TG has been used as a model drug to investigate the molecular events following MMR processing of chemotherapy drugs because its intracellular processing has been well studied. After 6-TG is taken up by cells, it is metabolically modified by hypoxanthine-guanine phosphoribosyl transferase (HPRT) to yield 6-thioguanosine monophosphate. Following subsequent phosphorylations, 6-thioguanosine triphosphate can then be incorporated into genomic DNA [6]. Incorporated 6-TG in the DNA is further chemically methylated by S-adenosylmethionine to form S6-methylthioguanine [7]. During subsequent DNA replication, S6-methylthioguanine can pair with thymine as well as its normal partner, cytosine. The resultant S6-methylthioguanine-thymine mispairs are identified and processed by MMR as replication errors [7]. MMR processing of 6-TG-induced mispairs occurs over several cell cycles and results in DNA single strand breaks [8], which may then activate a G₂/M cell cycle arrest followed by the induction of apoptosis and autophagy [4, 5, 8].

Macroautophagy (hereafter referred to as autophagy) is a catabolic process involving the degradation of a cell's own components through the lysosomal machinery [9]. During this process, part of the cytoplasm, including organelles such as mitochondria and long-lived proteins, are sequestered in a double-membrane vesicle, called an autophagosome. Then, the autophagosome delivers its contents to a lysosome to be degraded by lysosomal enzymes [9, 10]. Degradation and recycling of the contents of the vesicle enable the cell to continue to carry out essential processes for cell survival under stress conditions [11, 12]. However, prolonged autophagy results in type II (autophagic) programmed cell death [11].

Bcl2 and adenovirus E1B Nineteen-kilodalton Interacting Protein (BNIP3) is a Bcl-2 homology domain (BH3)-only protein in the Bcl-2 family [13]. BNIP3 mRNA and protein levels are upregulated through hypoxia-inducing factor-1-dependent and - independent mechanisms under stress conditions such as hypoxia [13, 14]. BNIP3 up-regulation has been

implicated in activation of apoptosis, autophagy, and necrosis, depending on the cell type and nature of the stimulus [13–15].

Checkpoints are present in all phases of the cell cycle and function to maintain the integrity of the genome [16]. Many clinically important chemotherapy drugs including 6-TG and 5-FU, which are used in this study, impart damage to the genome and activate cell cycle checkpoints [16–18]. Checkpoint kinase 1 (Chk1) is a key element in the DNA damage response pathway and plays a crucial role in the S-G₂/M-phase checkpoints. The G₂/M checkpoint prevents the cell from entering mitosis (M phase) if the genome is damaged [17, 18].

In our earlier reports, we showed that MMR machinery including MLH1 and MSH2 initiates 6-TG-induced autophagy in a p53 and mTOR-dependent manner [4, 5, 19]. In this study, we investigated the role of BNIP3 in mediating 6-TG- and 5-FU-induced autophagy and the relationship between a G₂/M cell cycle arrest and the activation of autophagy following MMR processing of these nucleoside analogs. We found that BNIP3 mediates induction of autophagy following p53 and mTOR activation as a result of MMR processing of both drugs. Our results also indicate that the activation of a G₂/M cell cycle arrest produces an inhibitory effect on the extent of autophagy after MMR-mediated drug processing.

Results

BNIP3 is required for induction of autophagy after DNA MMR processing of 6-TG and 5-FU

In our previous reports [4, 5], we used acridine orange staining, GFP-LC3 punctate dots, and LC3 immunoblot analysis to demonstrate that 6-TG induces a MMR-dependent autophagic response. To further confirm 6-TG-induced autophagy flux, we took advantage of a recently identified marker, p62/SQSTM1, for autophagic flux [20, 21]. After autophagy induction, p62/SQSTM1 binds directly to LC3 via a specific sequence motif and is itself degraded by autolysosomes after fusion of autophagosomes with lysosomes [20, 21]. Since p62 accumulates when autophagy degradation is blocked, and gets degraded when autophagy flux is induced, p62/SQSTM1 has been widely used as a marker to study autophagic flux [21]. As shown in Figure 1A, 6-TG treatment induces a dramatic decrease in p62/SQSTM1 levels in HCT116 (MLH1⁺, MMR⁺) cells, indicating that autophagic flux is induced instead of being blocked after 6-TG treatment.

To better understand the molecular mechanisms underlying MMR-initiated autophagy following 6-TG treatment as we reported earlier [4, 5, 19], we measured the protein levels of BNIP3 using immunoblot analysis with anti-BNIP3 antibodies. Three days after a 24h 6-TG treatment (when 6-TG induced autophagy peaks as shown below), we observed that BNIP3 protein levels are upregulated in HCT116 (MLH1⁺, MMR⁺) cells but not in HCT116 (MLH1⁻, MMR⁻) cells (Figure 1B). Consistently, BNIP3 mRNA dramatically increases after 6-TG treatment in HCT116 (MLH1⁺, MMR⁺) cells (Figure 1C). These data suggest that MMR mediates the up-regulation of BNIP3 following 6-TG treatment. Since multiple bands from immunoblot analysis with anti-BNIP3 antibodies were detected around 25 kDa, we next performed siRNA-mediated silencing of BNIP3 expression to determine the specificity of the antibodies against BNIP3. As shown in Figure 1D, BNIP3 knockdown

dramatically reduces signals from the multiple bands around 25 kDa, indicating that the antibodies against BNIP3 are specific. Since BNIP3 is implicated in promoting apoptosis [13–15], we then investigated whether or not a 6-TG-induced increase in BNIP3 expression affects induction of apoptosis. We found that siRNA-mediated silencing of BNIP3 expression does not impair 6-TG-induced Poly(ADP-ribose) Polymerase (PARP) cleavage, a marker of apoptosis [22], in HCT116 (MLH1⁺, MMR⁺) cells (Figure 1E).

We next questioned whether BNIP3 plays an essential role in MMR-initiated autophagy. As shown by the immunoblot in Figure 2A, siRNA-mediated suppression of BNIP3 expression (upper panel) markedly reduces a 6-TG-induced increase in the expression of LC3-II (lower panel), a specific marker of autophagy [23, 24], compared to control siRNA transfected cells. To confirm this result, we used another clinically active anti-cancer drug, 5-FU, which is also recognized and processed by MMR [25, 26]. As expected, BNIP3 knockdown (Figure 2B, upper panel) also dramatically inhibits the induction of autophagy following a 48h exposure to 5-FU (5 μ mol/L) as measured by LC3-II expression (Figure 2B, lower panel). Together, these data suggest that BNIP3 is essential for activation of autophagy after MMR processing of nucleoside analogs such as 6-TG and 5-FU.

Suppression of p53 expression impairs BNIP3 up-regulation following MMR processing of 6-TG and 5-FU

In our previous report [4], we showed that p53 mediates induction of autophagy after MMR processing of 6-TG. Here, we questioned whether p53 is required for the up-regulation of BNIP3 protein levels following MMR processing of 6-TG and 5-FU. In agreement with the 6-TG-induced up-regulation of BNIP3 protein levels as shown in Figure 1B, p53 is stabilized and activated in HCT116 (MLH1⁺, MMR⁺) cells but not in HCT116 (MLH1⁻, MMR⁻) cells following 6-TG treatment (Figure 3A). Furthermore, shRNA-mediated silencing of p53 expression (Figure 3B) abrogates a 6-TG-induced up-regulation of BNIP3 protein levels in HCT116 (MLH1⁺, MMR⁺) cells (Figure 3C). In agreement, p53 knockdown also impairs a 5-FU-induced increase in BNIP3 protein levels (Figure 3D). These data suggest that p53 is required for the up-regulation of BNIP3 protein levels following MMR processing of both 6-TG and 5-FU.

Rapamycin inhibition of mammalian target of rapamycin (mTOR) suppresses up-regulation of BNIP3 protein levels following MMR processing of 6-TG and 5-FU

Previously, we have also shown that mTOR positively regulates 6-TG-induced autophagy [19]. Here, we questioned whether mTOR affects the up-regulation of BNIP3 protein levels following MMR processing of 6-TG and/or 5-FU. As shown in Figure 4A, rapamycin cotreatment inhibits mTOR activity (upper panel) and subsequently reduces a 6-TG-induced increase in BNIP3 protein levels in a dose-dependent manner (lower panel), as measured by immunoblot analysis with anti-phospho-p70S6K (S6K1) (Thr³⁸⁹), a downstream target of activated mTOR [27, 28], and anti-BNIP3. Consistent with these results, rapamycin cotreatment also largely inhibits a 5-FU-induced increase in BNIP3 protein levels (Figure 4B, upper panel) and suppresses 5-FU-induced autophagy, as indicated by the decrease in the amount of LC3-II protein expression (Figure 4B, lower panel). Thus, these results

suggest that mTOR modulates the up-regulation of BNIP3 protein levels following MMR processing of both 6-TG and 5-FU.

Suppression of Chk1 expression promotes 6-TG-induced autophagy

To better understand the temporal relationship between a G₂/M cell cycle arrest and BNIP3-mediated autophagy after MMR processing of 6-TG, we measured the dynamic changes of these cellular responses. We treated HCT116 (MLH1⁺, MMR⁺) cells with 6-TG (3 μmol/L) for 24 hours and then monitored the temporal changes in the onset of G₂/M cell cycle arrest and apoptosis using propidium iodide staining and flow cytometry as well as autophagy using GFP-LC3 staining daily over a period of 5 days. Our results show that a G₂/M cell cycle arrest reached a peak at day 1 (Figure 5A). In agreement, our immunoblot analysis using anti-phospho-Chk1 (Ser³⁴⁵) showed that Chk1 activation also peaked at day 1 (Figure 5B), consistent with its role as an essential regulator of MMR-initiated G₂/M cell cycle arrest [29, 30]. In contrast, autophagy (Figure 5C) and apoptosis (Figure 5D) exhibited relatively late peak responses at day 3 after the 24h exposure to 6-TG in MMR⁺ cells. MMR⁻ cells did not show any changes in the G₂/M population nor in the extent of autophagy or apoptosis with 6-TG treatment compared to untreated MMR⁺ and MMR⁻ cells (data not shown).

To further determine whether a G₂/M cell cycle arrest affects the activation of 6-TG-induced autophagy in HCT116 (MLH1⁺, MMR⁺) cells, we performed siRNA-mediated silencing of Chk1 expression (Figure 6A) to inhibit the 6-TG-induced G₂/M cell cycle arrest. As shown in Figure 6B, suppression of Chk1 expression by Chk1 siRNA dramatically reduces a 6-TG-induced G₂/M cell cycle arrest. Interestingly, Chk1 knockdown largely promotes 6-TG-induced autophagy by three fold compared to control siRNA transfected cells (Figure 6C), indicating that the Chk1-mediated G₂/M cell cycle arrest produces an inhibitory effect on autophagy following MMR processing of 6-TG.

Discussion

DNA MMR is principally involved in correcting mismatches of the normal bases in the daughter strand which occur during scheduled and unscheduled DNA synthesis [1]. In addition, MMR mediates cytotoxicity of several classes of clinically active chemotherapy drugs including the nucleoside analogs, 6-TG- and 5-FU [1–3]. We previously reported that MMR initiates an autophagic response following 6-TG damage processing [4, 5], besides its well-known role in induction of apoptosis [1–3]. In this report, we continue to investigate the underlying molecular mechanisms leading to the activation of autophagy following MMR processing of 6-TG as well as 5-FU. We report that BNIP3 mediates MMR-initiated autophagy in a p53- and mTOR-dependent manner. We also show that the duration of a Chk1-activated G₂/M cell cycle arrest determines the level of autophagy following MMR processing of 6-TG.

Increased expression of BNIP3 has been implicated in apoptosis, autophagy, and necrosis [13–15]. Surprisingly, our results show that siRNA knockdown of BNIP3 enhances 6-TG-induced cleavage of PARP (Figure 1E), a marker of apoptosis. However, we also found that BNIP3 plays an essential role in mediating 6-TG and 5-FU-induced autophagy (Figure 2).

These data suggest that siRNA inhibition of BNIP3 and then autophagy inhibits apoptosis after MMR processing of 6-TG. The underlying mechanism may be that 6-TG-induced autophagy degrades damaged mitochondria with loss of membrane potential and, thus, eliminates the triggers of apoptosis [31].

The expression of BNIP3 is reported to be tightly regulated as its overexpression induces cell death [13, 14]. Under hypoxic conditions, the hypoxia-inducing factor-1 (HIF-1) is stabilized and accumulates to function as a transcription factor to induce expression of multiple genes, including BNIP3 [13, 14]. In response to hypoxia, stabilization of p53 also ensues, but BNIP3 up-regulation under hypoxia was found to be independent of p53 [14]. However, in our study, the up-regulation of BNIP3 protein levels depends on p53 activation as a consequence of MMR processing of 6-TG and 5-FU (Figure 3). Since p53 usually functions as a transcription factor and BNIP3L, a BNIP3 homologue, is regulated by p53 at the transcriptional level [32], we are currently attempting to determine whether p53 increases BNIP3 expression through regulating BNIP3 promoter activity.

Extensive studies have described that rapamycin inhibits mTOR, a negative regulator of autophagy, and then activates autophagy in mammalian cells [33, 34]. Recent reports further suggest that, under nutrient-rich conditions, mTOR inhibits autophagy probably through its association with the protein complex, ULK1-mAtg13-FIP200, and phosphorylation of ULK1 and mAtg13 on sites that inhibit their activity [35, 36]. Under starvation conditions, mTOR dissociates from the ULK1-mAtg13-FIP200 complex, inducing ULK1 to become active and phosphorylate mAtg13 and FIP200, thus promoting the translocation of the protein complex to sites of autophagosome formation [35, 36]. However, some recent studies have shown that autophagy can also be induced in a mTOR-independent manner [37, 38]. Previously we reported that mTOR inhibition by rapamycin and siRNA knockdown of S6K1, one of mTOR downstream effector, inhibit 6-TG-induced autophagy [19]. We further found that mTOR inhibition by rapamycin activates Akt, probably through relieving the negative feedback inhibition by mTOR-S6K1 [19]. Activated Akt resulting from mTOR inhibition by rapamycin may phosphorylate and inactivate its substrates such as Foxo, which has recently been found to be involved in autophagy in *Drosophila* [39] and mouse skeletal muscle [40]. Here, we also show that mTOR modulates the up-regulation of BNIP3 protein levels following MMR processing of 6-TG and 5-FU (Figure 4). Although the mechanism is still not well understood, activated S6K1 by mTOR has been reported to participate in protein synthesis [41, 42]. Therefore, our data, as presented in Figure 4, suggest that mTOR-S6K1 may also control BNIP3 protein translation and play a positive role in regulating 6-TG-induced autophagy. After MMR processing of 6-TG or 5-FU, the effect of BNIP3 on mediating induction of autophagy may be dominant over the negative effect of mTOR as discussed above. This may also explain why mTOR inhibition by rapamycin inhibits 6-TG or 5-FU-induced autophagy instead of activating autophagy.

When BNIP3 expression is induced by certain stress stimuli, it localizes to the mitochondria through its transmembrane domain. This domain integrates into the outer membrane of the mitochondria; thereby resulting in opening of the permeability transition (PT) pore, loss of mitochondrial membrane potential (Ψ_m) and increase in production of reactive oxygen species (ROS) [13–15]. ROS have been implicated as a critical trigger of activation of

autophagy [14, 43]. Therefore, we speculate that following initiation of MMR processing of chemotherapy drugs such as 6-TG and 5-FU, p53 is activated and functions as a transcription factor to upregulate BNIP3 transcription, while mTOR-S6K1 modulates BNIP3 protein translation. The upregulated BNIP3 disturbs mitochondrial function, subsequently increases production of ROS, and then mediates the activation of autophagy as a consequence of MMR processing of 6-TG and 5-FU. Experiments are planned to test these hypotheses.

In this study, we also show that a Chk1-activated G₂/M cell cycle arrest produces an inhibitory effect on 6-TG-induced autophagy and apoptosis following MMR processing (Figure 6). These data suggest that if chemical inhibitors are developed and used to inhibit Chk1 activity (e.g. UCN-01), synergistic cytotoxic effects of MMR-processing of nucleoside analogs such as 5-FU and 6-TG combined with Chk1 inhibitors may result [44].

In conclusion, we show that BNIP3 plays an essential role in mediating the induction of autophagy in a p53- and mTOR-dependent manner following MMR processing of 6-TG and 5-FU. Our results also indicate that the Chk1-activated G₂/M cell cycle arrest produces an inhibitory effect on the extent of autophagy following MMR processing of 6-TG.

Materials and Methods

Cell culture

Human colorectal cancer (HCT116) cells are MMR-deficient (MLH1⁻, MMR⁻) because the *hMLH1* gene in these cells contains a base substitution that results in a termination signal at codon 252°(TCA→TAA) [45]. HCT116 cells with stable transfection of human MLH1 cDNA to restore MMR activity (MLH1⁺, MMR⁺) in the HCT116 cells as well as the empty vector control HCT116 cells (MLH1⁻, MMR⁻) were kindly provided by Dr. Françoise Praz (Centre National de la Recherche Scientifique, Villejuif, France) [46]. The cells were maintained in Dulbecco's Modification of Eagle's Medium (DMEM) (Mediatech, Inc, Herndon, VA) and supplemented with 10% FBS (Hyclone, Logan, UT), penicillin (100µg/ml), streptomycin (100 units/ml), L-glutamine (2 mmol/L) and nonessential amino acids (0.1 mmol/L) (Invitrogen, Carlsbad, CA).

Drug treatment

Cells were seeded at 30,000 cells/60-mm dish and allowed to attach and grow for ~17–18h prior to drug treatments. Based on preliminary experiments and prior published data [3–5, 9, 25, 26], cells were exposed to 3 µmol/L 6-TG for 24 h or 5µmol/L 5-FU for 48h (Sigma-Aldrich, St. Louis, MO), after which cells were incubated in drug-free medium for up to 5 days. To assess the effects of inhibition of mTOR on 6-TG MMR processing, HCT116 (MLH1⁺, MMR⁺) cells were treated with 6-TG (3 µmol/L × 24h) and then treated with various concentrations of rapamycin (EMD Chemicals, Inc., Gibbstown, NJ) (0, 0.2, 1.0, or 5.0 nmol/L) for 3 days prior to analysis. To assess the effect of inhibition of mTOR on 5-FU MMR processing, HCT116 (MLH1⁺, MMR⁺) cells were co-treated with 5 µmol/L 5-FU and 5 nmol/L rapamycin for 48h prior to analyses.

Stable transfection of GFP-LC3 in HCT116 cells

HCT116 (MLH1⁺, MMR⁺) cells with stable expression of GFP-LC3 were generated, as we described previously [4]. pGFP-LC3 plasmids were kindly provided by Dr. Tamotsu Yoshimori (National Institute of Genetics, Shizuoka-ken, Japan) [23].

RNA interference (RNAi)-mediated gene silencing of BNIP3, Chk1 and p53 expression

Small-interfering (siRNA) oligos were chemically synthesized by Dharmacon, Inc (Lafayette, Colorado). The siRNA sequence specific for luciferase (cont: 5'-CGUACGCGGAAUACUUCGAdTdT-3') was used as a control. The sense siRNA sequences for knocking down BNIP3 and Chk1 are: 5'-AAGGAACACGAGCGUCAUGAAdTdT-3' (BNIP3) and 5'-GCGUGCCGUAGACUGUCCAdTdT-3' (Chk1). siRNAs were transfected using LipofectAMINE 2000 (Invitrogen), according to the manufacturer's protocol. Small hairpin RNA (shRNA)-mediated stable silencing of p53 in HCT116 (MLH1⁺, MMR⁺) cells was performed, as we described previously [4].

Quantitative real-time polymerase chain reaction

Total RNA was isolated using the RNeasy[®] Mini Kit (Qiagen, Valencia, CA). Quantitative real-time polymerase chain reactions were performed in triplicate for each sample on a 7500 Real-Time PCR System (Applied Biosystems, Foster City, CA). The thermocycling conditions were: initial 10 min incubation at 95°C followed by 40 cycles of denaturation for 15 s at 95°C and extension/annealing for 1 min at 60°C. PCR data were collected and analyzed using Sequence Detection System (SDS) software. PCR primers used for BNIP3 gene are: 5'-GCCACCTCGCTCGCAGACAC-3' (forward) and 5'-CAATCCGATGGCCAGCAAATGAGA-3' (reverse). Relative quantitation of BNIP3 mRNAs was performed by the comparative Ct method [47]. The expression levels of BNIP3 mRNA are normalized to those of the endogenous control 18S rRNA and the mean Ct obtained in untreated cells for BNIP3 mRNA was used as calibrator. The relative quantitation values were plotted on a log₁₀ scale.

Propidium iodide staining for analysis of cell cycle and apoptosis

Cells were fixed with 90% ethanol at -20°C for 15 minutes, incubated with RNase, stained with propidium iodide (Sigma-Aldrich), and then subjected to flow cytometry (Epics XL-MCL, Beckman Coulter, Inc.). Flow cytometric data were analyzed with Modfit 3.0 (Verity Software, Topsham, ME).

Western Blotting

SDS-PAGE and immunoblot analyses were carried out, as described previously [4]. The primary antibodies used for immunoblot analyses included: rabbit polyclonal antibodies against LC3 kindly provided by Dr. Tamotsu Yoshimori (National Institute of Genetics, Shizuoka-ken, Japan) [23] or purchased from Abcam Inc (Cambridge, MA); rabbit polyclonal antibodies against cleaved PARP (Promega, Madison, WI); rabbit monoclonal antibodies against phospho-Chk1 (Ser³⁴⁵) and mouse monoclonal antibodies against phospho-S6K1 (Thr³⁸⁹) (Cell Signaling Technology, Inc., Danvers, MA); mouse polyclonal

antibodies against p62/SQSTM1 (Abnova, Taipei, Taiwan) and mouse monoclonal antibodies against β -Actin and α -Tubulin (Sigma-Aldrich), p53 (Santa Cruz Biotechnology, Inc., Santa Cruz, CA) and BNIP3 (Abcam Inc).

Acknowledgements

We thank Drs. Francoise Praz for providing the cell systems used in this study, Dr. Tamotsu Yoshimori for providing the antibody against LC3 and pEGFP-LC3 plasmids and all the members of the Kinsella laboratory for their helpful discussions.

Supported by NIH grant U56 CA112963, the DBJ Foundation, the Richard A. Green Foundation and the University Radiation Medicine Foundation.

References

1. Modrich P, Lahue R. Mismatch repair in replication fidelity, genetic recombination, and cancer biology. *Annu Rev Biochem.* 1996; 65:101–133. [PubMed: 8811176]
2. Stojic L, Brun R, Jiricny J. Mismatch repair and DNA damage signalling. *DNA Repair (Amst).* 2004; 3:1091–1101. [PubMed: 15279797]
3. Fink D, Aebi S, Howell SB. The role of DNA mismatch repair in drug resistance. *Clin Cancer Res.* 1998; 4:1–6. [PubMed: 9516945]
4. Zeng X, Yan T, Schupp JE, Seo Y, Kinsella TJ. DNA mismatch repair initiates 6-thioguanine-induced autophagy through p53 activation in human tumor cells. *Clin Cancer Res.* 2007; 13:1315–1321. [PubMed: 17317843]
5. Zeng X, Kinsella TJ. A novel role for DNA mismatch repair and the autophagic processing of chemotherapy drugs in human tumor cells. *Autophagy.* 2007; 3:368–370. [PubMed: 17426439]
6. Elion GB. The purine path to chemotherapy. *Science.* 1989; 244:41–47. [PubMed: 2649979]
7. Swann PF, Waters TR, Moulton DC, et al. Role of postreplicative DNA mismatch repair in the cytotoxic action of thioguanine. *Science.* 1996; 273:1109–1111. [PubMed: 8688098]
8. Yan T, Berry SE, Desai AB, Kinsella TJ. DNA mismatch repair (MMR) mediates 6-thioguanine genotoxicity by introducing single-strand breaks to signal a G2-M arrest in MMR-proficient RKO cells. *Clin Cancer Res.* 2003; 9:2327–2334. [PubMed: 12796402]
9. Seglen PO, Bohley P. Autophagy and other vacuolar protein degradation mechanisms. *Experientia.* 1992; 48:158–172. [PubMed: 1740188]
10. Dunn WA Jr. Studies on the mechanisms of autophagy: maturation of the autophagic vacuole. *J Cell Biol.* 1990; 110:1935–1945. [PubMed: 2161853]
11. Shintani T, Klionsky DJ. Autophagy in health and disease: a double-edged sword. *Science.* 2004; 306:990–995. [PubMed: 15528435]
12. Hait WN, Jin S, Yang JM. A matter of life or death (or both): understanding autophagy in cancer. *Clin Cancer Res.* 2006; 12:1961–1965. [PubMed: 16609004]
13. Zhang J, Ney PA. Role of BNIP3 and NIX in cell death, autophagy, and mitophagy. *Cell Death Differ.* 2009; 16:939–946. [PubMed: 19229244]
14. Burton TR, Gibson SB. The role of Bcl-2 family member BNIP3 in cell death and disease: NIPping at the heels of cell death. *Cell Death Differ.* 2009; 16:515–523. [PubMed: 19136941]
15. Daido S, Kanzawa T, Yamamoto A, Takeuchi H, Kondo Y, Kondo S. Pivotal role of the cell death factor BNIP3 in ceramide-induced autophagic cell death in malignant glioma cells. *Cancer Res.* 2004; 64:4286–4293. [PubMed: 15205343]
16. Canman CE. Replication checkpoint: preventing mitotic catastrophe. *Curr Biol.* 2001; 11:R121–R124. [PubMed: 11250164]
17. Rhind N, Russell P. Chk1 and Cds1: linchpins of the DNA damage and replication checkpoint pathways. *J Cell Sci.* 2000; 113(Pt 22):3889–3896. [PubMed: 11058076]
18. Enders GH. Expanded roles for Chk1 in genome maintenance. *J Biol Chem.* 2008; 283:17749–17752. [PubMed: 18424430]

19. Zeng X, Kinsella TJ. Mammalian target of rapamycin and S6 kinase 1 positively regulate 6-thioguanine-induced autophagy. *Cancer Res.* 2008; 68:2384–2390. [PubMed: 18381446]
20. Pankiv S, Clausen TH, Lamark T, et al. p62/SQSTM1 binds directly to Atg8/LC3 to facilitate degradation of ubiquitinated protein aggregates by autophagy. *J Biol Chem.* 2007; 282:24131–24145. [PubMed: 17580304]
21. Bjorkoy G, Lamark T, Pankiv S, Overvatn A, Brech A, Johansen T. Monitoring autophagic degradation of p62/SQSTM1. *Methods Enzymol.* 2009; 452:181–197. [PubMed: 19200883]
22. Oliver FJ, de la Rubia G, Rolli V, Ruiz-Ruiz MC, de Murcia G, Murcia JM. Importance of poly(ADP-ribose) polymerase and its cleavage in apoptosis. Lesson from an uncleavable mutant. *J Biol Chem.* 1998; 273:33533–33539. [PubMed: 9837934]
23. Kabeya Y, Mizushima N, Ueno T, et al. LC3, a mammalian homologue of yeast Apg8p, is localized in autophagosomal membranes after processing. *Embo J.* 2000; 19:5720–5728. [PubMed: 11060023]
24. Mizushima N. Methods for monitoring autophagy. *Int J Biochem Cell Biol.* 2004; 36:2491–2502. [PubMed: 15325587]
25. Meyers M, Wagner MW, Hwang HS, Kinsella TJ, Boothman DA. Role of the hMLH1 DNA mismatch repair protein in fluoropyrimidine-mediated cell death and cell cycle responses. *Cancer Res.* 2001; 61:5193–5201. [PubMed: 11431359]
26. Tajima A, Hess MT, Cabrera BL, Kolodner RD, Carethers JM. The mismatch repair complex hMutS alpha recognizes 5-fluorouracil-modified DNA: implications for chemosensitivity and resistance. *Gastroenterology.* 2004; 127:1678–1684. [PubMed: 15578504]
27. Peterson TR, Sabatini DM. eIF3: a connectOR of S6K1 to the translation preinitiation complex. *Mol Cell.* 2005; 20:655–657. [PubMed: 16337588]
28. Nobukuni T, Kozma SC, Thomas G. hvps34, an ancient player, enters a growing game: mTOR Complex1/S6K1 signaling. *Curr Opin Cell Biol.* 2007; 19:135–141. [PubMed: 17321123]
29. Yan T, Desai AB, Jacobberger JW, Sramkoski RM, Loh T, Kinsella TJ. CHK1 and CHK2 are differentially involved in mismatch repair-mediated 6-thioguanine-induced cell cycle checkpoint responses. *Mol Cancer Ther.* 2004; 3:1147–1157. [PubMed: 15367709]
30. Yamane K, Taylor K, Kinsella TJ. Mismatch repair-mediated G2/M arrest by 6-thioguanine involves the ATR-Chk1 pathway. *Biochem Biophys Res Commun.* 2004; 318:297–302. [PubMed: 15110787]
31. Herman-Antosiewicz A, Johnson DE, Singh SV. Sulforaphane causes autophagy to inhibit release of cytochrome C and apoptosis in human prostate cancer cells. *Cancer Res.* 2006; 66:5828–5835. [PubMed: 16740722]
32. Fei P, Wang W, Kim SH, et al. Bnip3L is induced by p53 under hypoxia, and its knockdown promotes tumor growth. *Cancer Cell.* 2004; 6:597–609. [PubMed: 15607964]
33. Yorimitsu T, Klionsky DJ. Autophagy: molecular machinery for self-eating. *Cell Death Differ.* 2005; 12:1524–1552.
34. Rubinsztein DC, Gestwicki JE, Murphy LO, Klionsky DJ. Potential therapeutic applications of autophagy. *Nat Rev Drug Discov.* 2007; 6:304–312. [PubMed: 17396135]
35. Hosokawa N, Hara T, Kaizuka T, et al. Nutrient-dependent mTORC1 association with the ULK1-Atg13-FIP200 complex required for autophagy. *Mol Biol Cell.* 2009; 20:1981–1991. [PubMed: 19211835]
36. Chan EY. mTORC1 phosphorylates the ULK1-mAtg13-FIP200 autophagy regulatory complex. *Sci Signal.* 2009; 2:pe51. [PubMed: 19690328]
37. Sarkar S, Floto RA, Berger Z, et al. Lithium induces autophagy by inhibiting inositol monophosphatase. *J Cell Biol.* 2005; 170:1101–1111. [PubMed: 16186256]
38. Sarkar S, Davies JE, Huang Z, Tunnacliffe A, Rubinsztein DC. Trehalose, a novel mTOR-independent autophagy enhancer, accelerates the clearance of mutant huntingtin and alpha-synuclein. *J Biol Chem.* 2007; 282:5641–5652. [PubMed: 17182613]
39. Juhasz G, Puskas LG, Komonyi O, et al. Gene expression profiling identifies FKBP39 as an inhibitor of autophagy in larval *Drosophila* fat body. *Cell Death Differ.* 2007; 14:1181–1190. [PubMed: 17363962]

40. Mammucari C, Milan G, Romanello V, et al. FoxO3 controls autophagy in skeletal muscle in vivo. *Cell Metab.* 2007; 6:458–471. [PubMed: 18054315]
41. Schmelzle T, Hall MN. TOR, a central controller of cell growth. *Cell.* 2000; 103:253–262. [PubMed: 11057898]
42. Sabatini DM. mTOR and cancer: insights into a complex relationship. *Nat Rev Cancer.* 2006; 6:729–734. [PubMed: 16915295]
43. Liu Z, Lenardo MJ. Reactive oxygen species regulate autophagy through redox-sensitive proteases. *Dev Cell.* 2007; 12:484–485. [PubMed: 17419989]
44. Ashwell S, Janetka JW, Zabludoff S. Keeping checkpoint kinases in line: new selective inhibitors in clinical trials. *Expert Opin Investig Drugs.* 2008; 17:1331–1340.
45. Papadopoulos N, Nicolaides NC, Wei YF, et al. Mutation of a mutL homolog in hereditary colon cancer. *Science.* 1994; 263:1625–1629. [PubMed: 8128251]
46. Jacob S, Aguado M, Fallik D, Praz F. The role of the DNA mismatch repair system in the cytotoxicity of the topoisomerase inhibitors camptothecin and etoposide to human colorectal cancer cells. *Cancer Res.* 2001; 61:6555–6562. [PubMed: 11522654]
47. Livak KJ, Schmittgen TD. Analysis of relative gene expression data using real-time quantitative PCR and the 2⁻($\Delta\Delta C(T)$) Method. *Methods.* 2001; 25:402–408. [PubMed: 11846609]

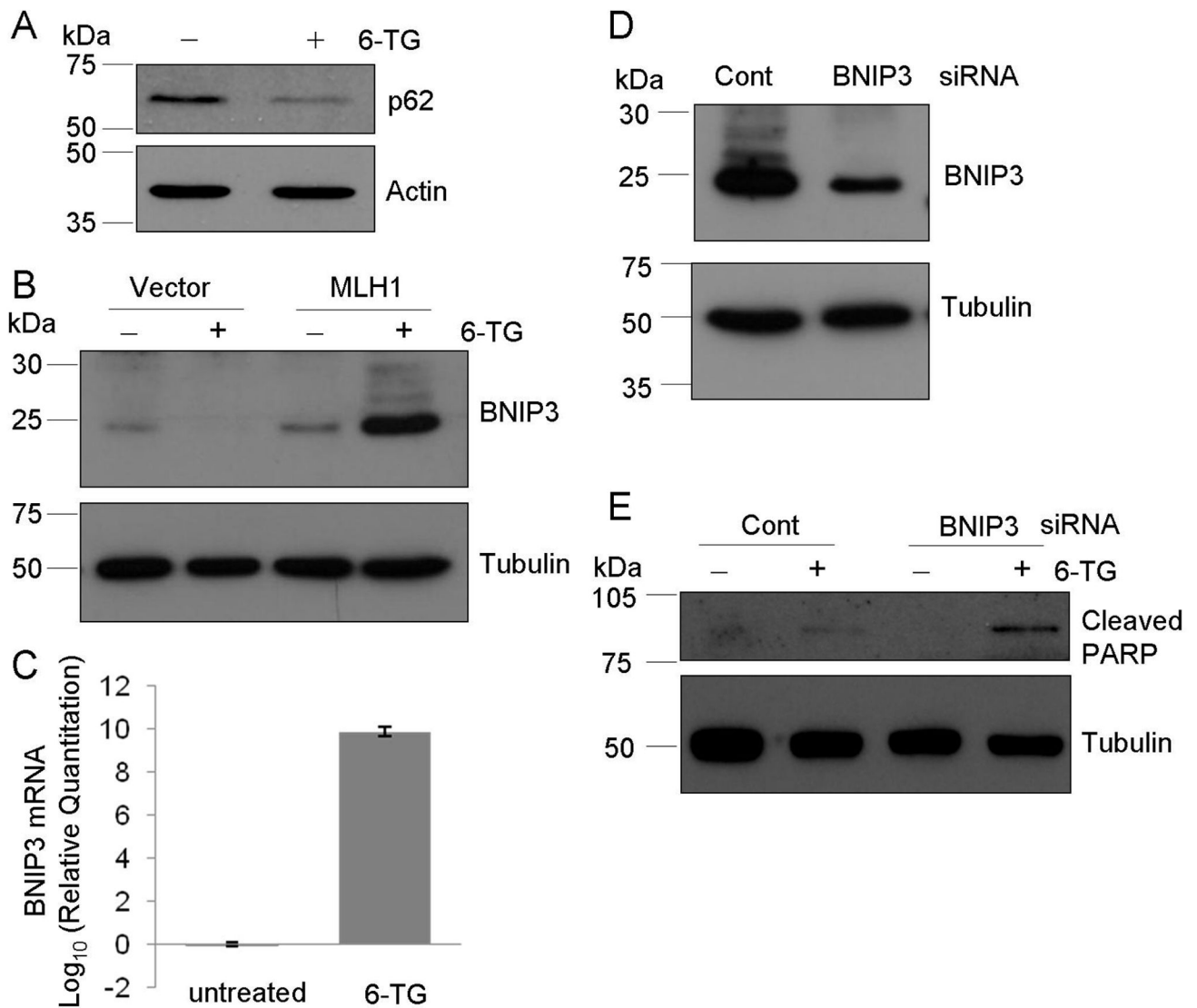


Figure 1. BNIP3 protein levels are upregulated in a MMR-dependent manner in response to 6-TG

(A) HCT116 cells stably transfected with MLH1 cDNA (MLH1⁺, MMR⁺) were treated with 3 μ mol/L 6-TG for 24 h, harvested, and subjected to immunoblot analysis with antibodies against p62/SQSTM1 at day 3 after 6-TG treatment. (B) HCT116 cells stably transfected with an empty vector (MLH1⁻, MMR⁻) or with MLH1 cDNA (MLH1⁺, MMR⁺) were treated with 3 μ mol/L 6-TG for 24 h, harvested, and subjected to immunoblot analysis with antibodies against BNIP3 at day 3 after 6-TG treatment. (C) HCT116 (MLH1⁺, MMR⁺) cells were treated with 3 μ mol/L 6-TG for 24 h. Total RNA was isolated at day 3 after 6-TG treatment. Quantitative real-time PCR was then performed as described in the Materials and Methods. The expression levels of BNIP3 mRNA were normalized to those of the endogenous control 18S rRNA and the mean Ct obtained in untreated cells for BNIP3 mRNA was used as calibrator. The relative quantitation values from triplicate reactions were

plotted on a \log_{10} scale as mean \pm standard error. **(D)** HCT116 (MLH1⁺, MMR⁺) cells were transfected with control luciferase (cont) or BNIP3 siRNA oligos, as described in the Materials and Methods. Two days after the siRNA transfection, the cells were harvested and analyzed by immunoblot analysis with antibodies against BNIP3. **(E)** HCT116 (MLH1⁺, MMR⁺) cells were treated with 3 $\mu\text{mol/L}$ 6-TG for 24 h, harvested, and subjected to immunoblot analysis with antibodies against cleaved PARP at day 3 after 6-TG treatment.

Author Manuscript

Author Manuscript

Author Manuscript

Author Manuscript

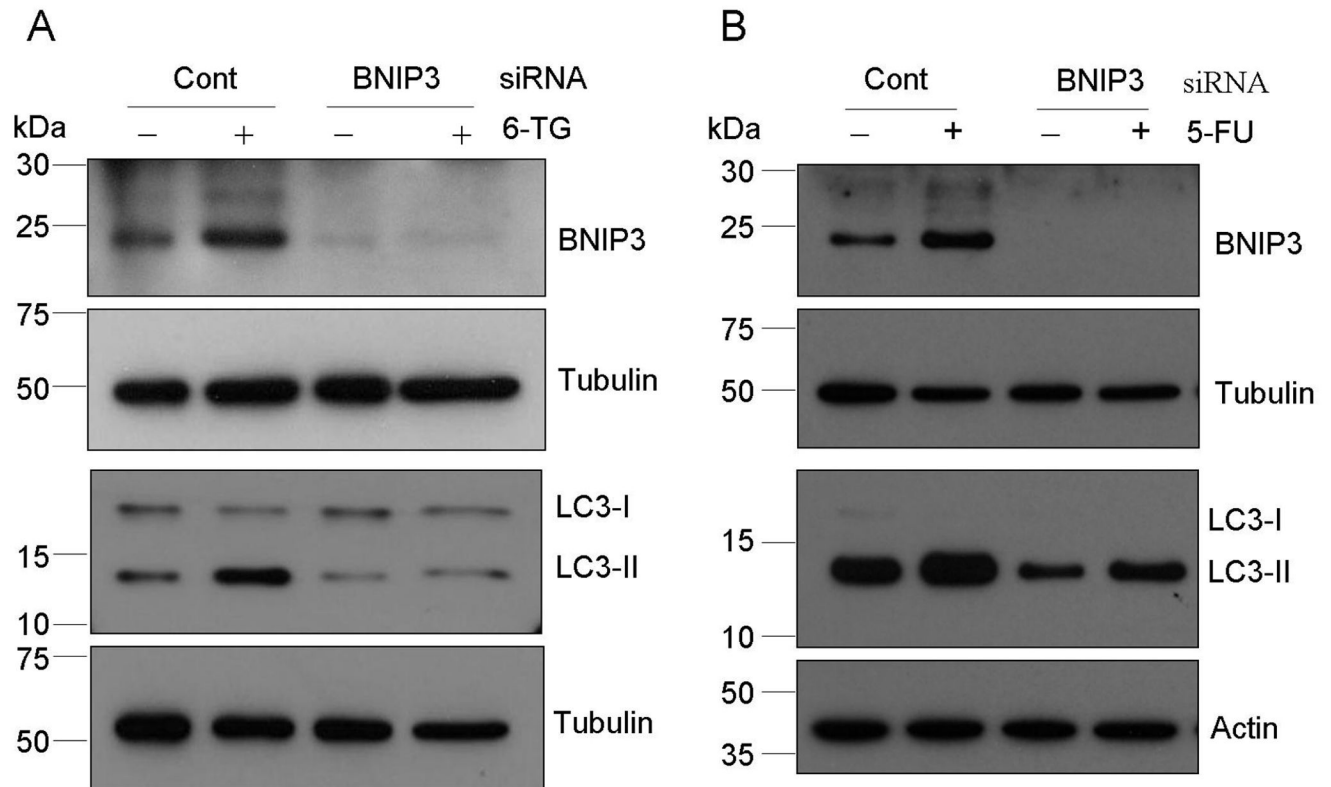


Figure 2. siRNA-mediated silencing of BNIP3 expression impairs 6-TG and 5-FU-induced autophagy

(**A**) HCT116 (MLH1⁺, MMR⁺) cells were treated with 3 μ mol/L 6-TG for 24h. Control luciferase (cont) or BNIP3 siRNA oligos were then transfected into the cells, as described in the Materials and Methods. At day 3 after exposure to 6-TG, the cells were harvested and analyzed by immunoblot analysis with antibodies against BNIP3 (upper panel) and LC3 (lower panel). (**B**) Control luciferase (cont) or BNIP3 siRNA oligos were transfected into HCT116 (MLH1⁺, MMR⁺) cells, as described above. The cells were then incubated with 5 μ mol/L 5-FU for 48h, harvested and subjected to SDS-PAGE and immunoblot analysis with anti-BNIP3 (upper panel) and anti-LC3 (lower panel).

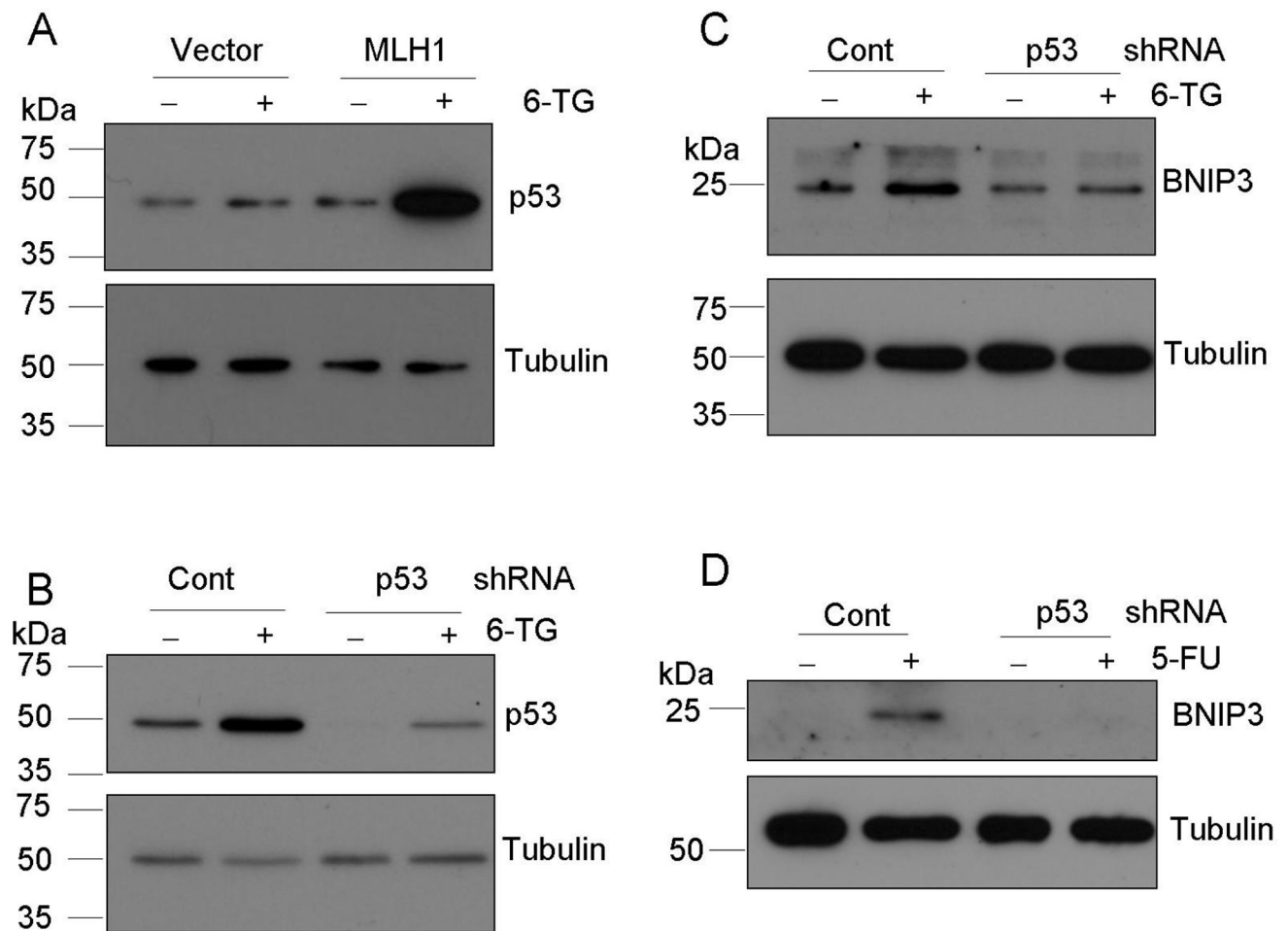


Figure 3. shRNA-mediated suppression of p53 expression abrogates 6-TG and 5-FU-induced up-regulation of BNIP3 protein levels

(A) HCT116 cells stably transfected with an empty vector (MLH1⁻, MMR⁻) or with MLH1 cDNA (MLH1⁺, MMR⁺) were treated with 3 $\mu\text{mol/L}$ 6-TG for 24h, harvested, and subjected to immunoblot analysis with antibodies against p53 at day 3 after 6-TG treatment. (B) small hairpin RNA-mediated stable silencing of p53 expression was performed, as described in the Materials and Methods. p53 expression was tested by immunoblot analysis with anti-p53. Control and p53 knockdown HCT116 (MLH1⁺, MMR⁺) cells were then treated with 3 $\mu\text{mol/L}$ 6-TG for 24 h (C) or 5 $\mu\text{mol/L}$ 5-FU for 48 h (D). 72h after 6-TG exposure or 48h after 5-FU addition, the cells were harvested and subjected to SDS-PAGE and immunoblot analysis with anti-BNIP3.

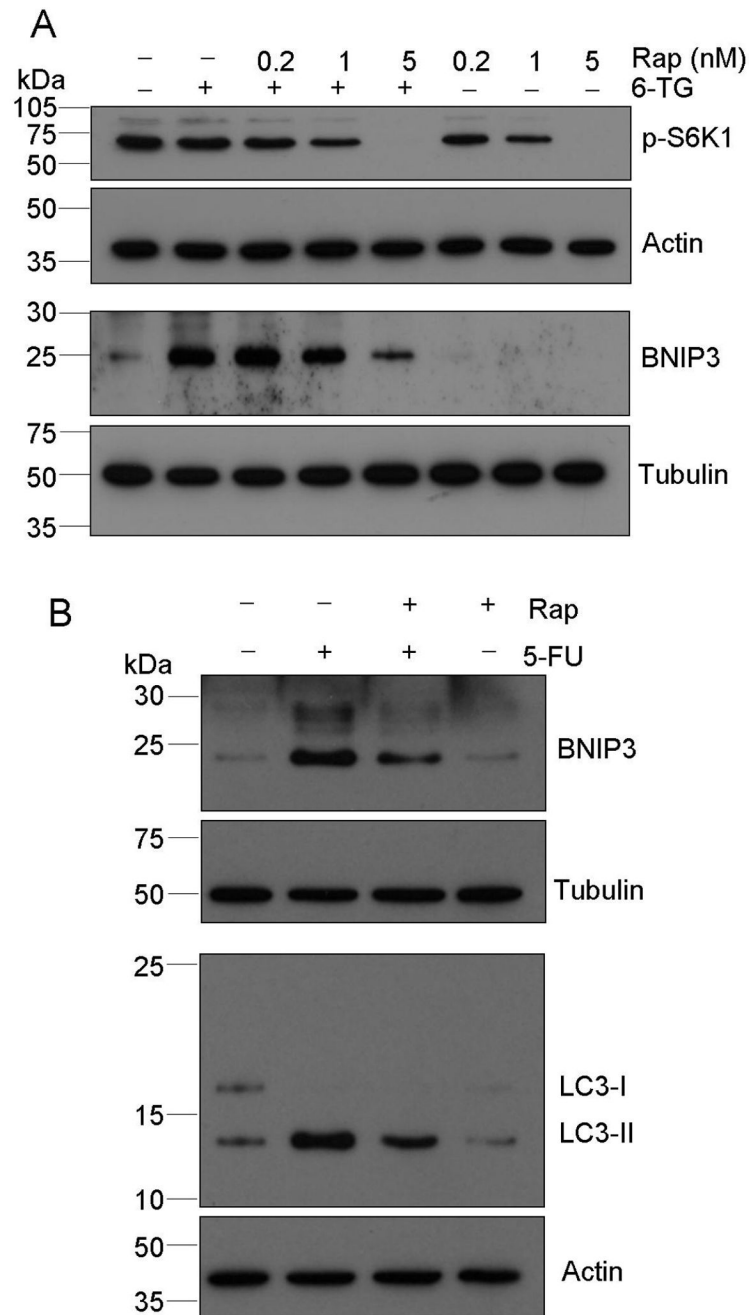


Figure 4. Inhibition of mTOR by rapamycin impairs 6-TG and 5-FU-induced up-regulation of BNIP3 protein levels

(A) HCT116 (MLH1⁺, MMR⁺) cells were treated with 3 μ mol/L 6-TG for 24h. Then, 0, 0.2, 1, or 5 nmol/L rapamycin was added for another 3d to inhibit mTOR activity. At day 3 after exposure to 6-TG, cells were harvested and analyzed by immunoblot analysis with antibodies against phospho-p70S6K (S6K1) (Thr³⁸⁹) (upper panel) and BNIP3 (lower panel). (B) HCT116 (MLH1⁺, MMR⁺) cells were cotreated with 5 μ mol/L 5-FU and 5 nmol/L rapamycin for 48h. The treated cells were harvested and analyzed by immunoblot analysis with anti-BNIP3 (upper panel) and anti-LC3 (lower panel).

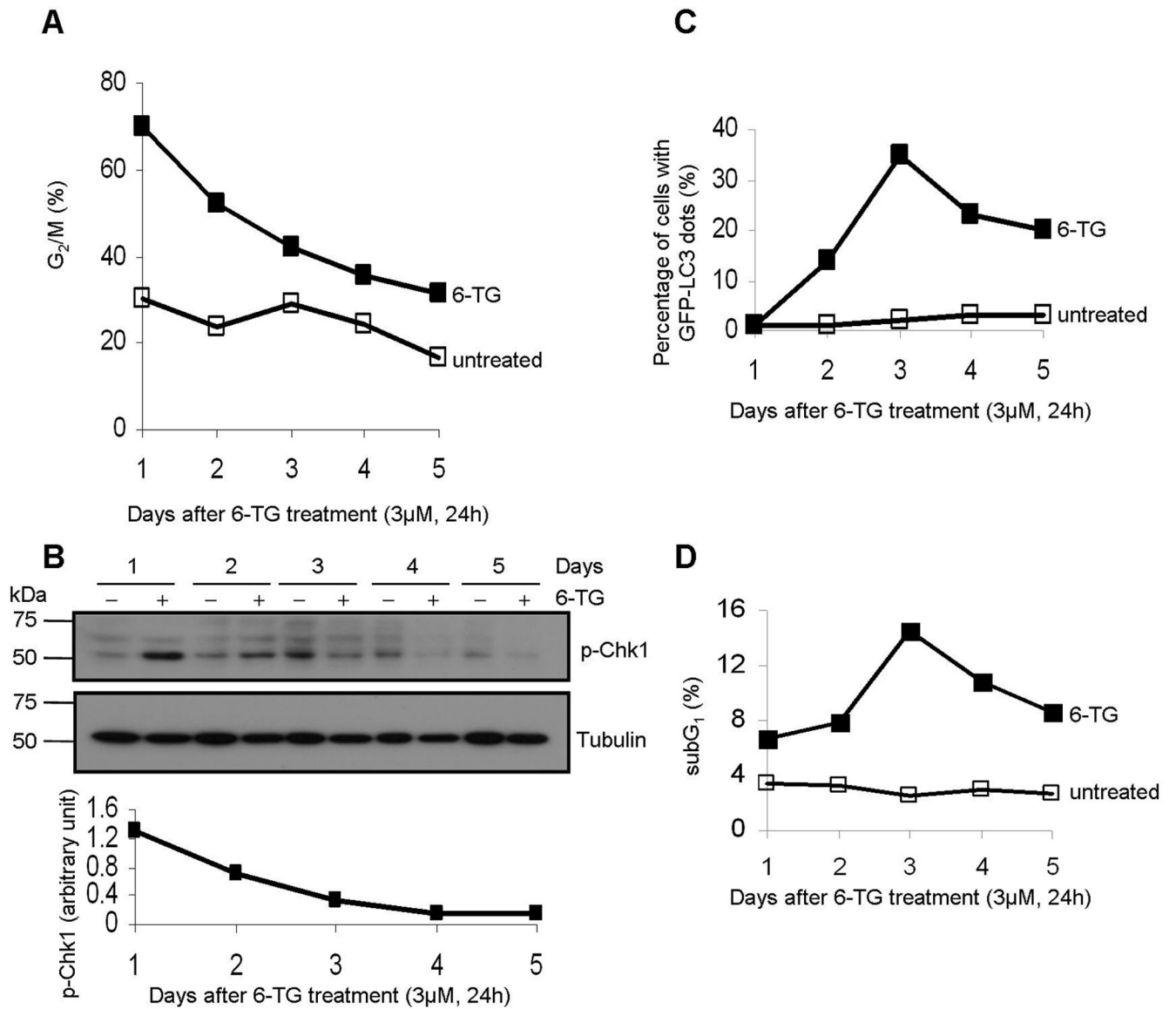


Figure 5. 6-TG induces a G₂/M cell cycle arrest peaking at day 1 while activation of autophagy and apoptosis exhibits a peak response at day 3 in MMR⁺ cells

HCT116 (MLH1⁺, MMR⁺) cells were treated with 3 μmol/L 6-TG for 24h. The cells were then harvested and stained with propidium iodide for cell cycle analysis (A), as described in the Materials and Methods, or subjected to immunoblot analysis with anti-phospho-Chk1 (Ser³⁴⁵) (B) daily for up to 5d after 6-TG treatment. The amount of phospho-Chk1 (Ser³⁴⁵) and tubulin was quantified using NIH Image J and the ratio of phospho-Chk1 (Ser³⁴⁵) to tubulin following 6-TG treatment was graphed in the lower panel. (C) HCT116 (MLH1⁺, MMR⁺) cells were stably transfected with pGFP-LC3, as described in the Materials and Methods. The GFP-LC3-expressing cells were treated with 3 μmol/L 6-TG for 24h. The cells were examined under fluorescence microscopy and the percentage of GFP-LC3-positive cells with GFP-LC3 punctate dots was determined for up to 5d after 6-TG

treatment. A minimum of 250 cells per sample was counted. **(D)** HCT116 (MLH1⁺, MMR⁺) cells were treated with 3 $\mu\text{mol/L}$ 6-TG for 24h. The cells were then harvested, stained with propidium iodide, and then subjected to flow cytometry for DNA content analysis as described above. The percentage of cells in subG₁ was then graphed. *Open square*, untreated; *closed square*, 6-TG treated.

Author Manuscript

Author Manuscript

Author Manuscript

Author Manuscript

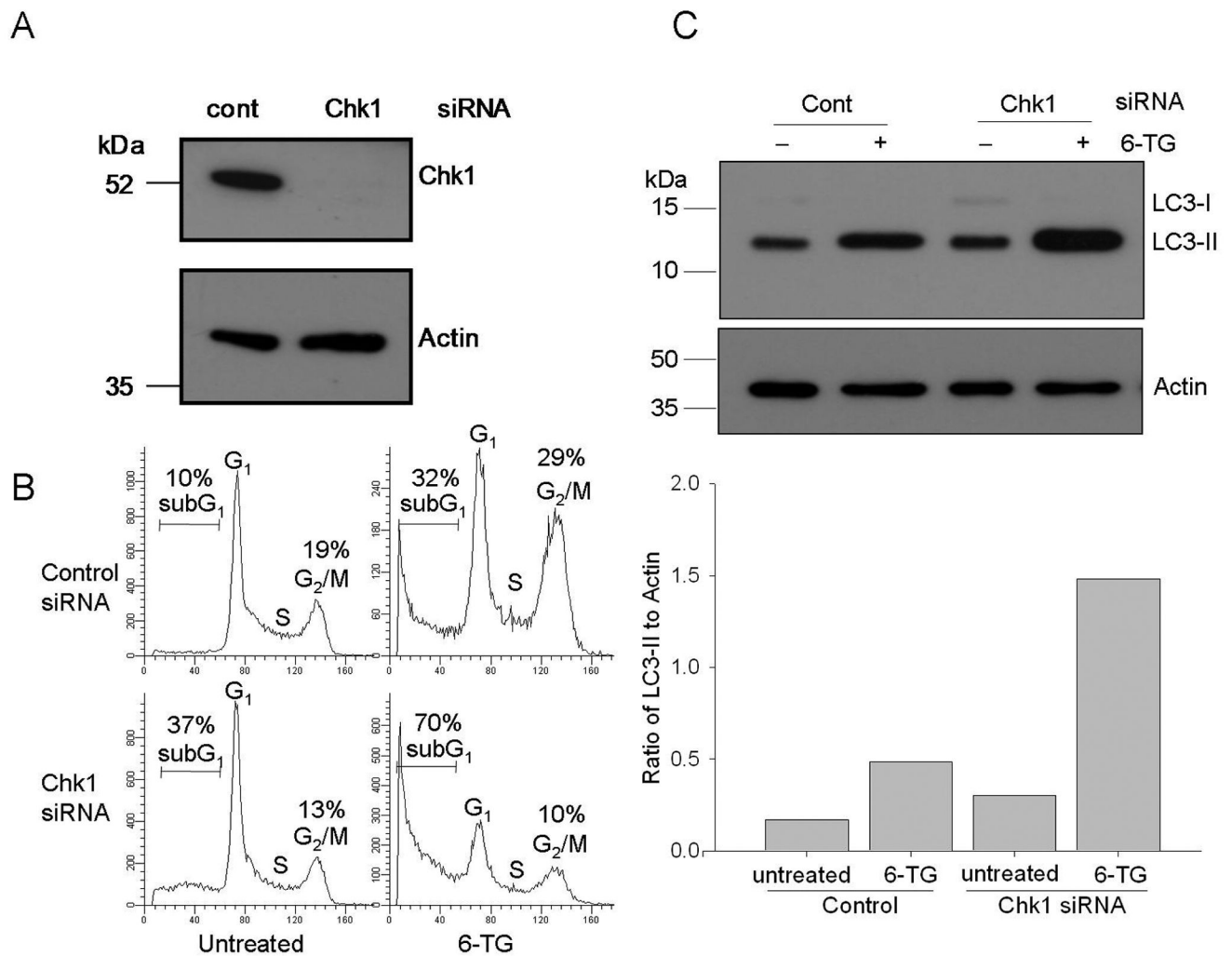


Figure 6. siRNA-mediated silencing of Chk1 expression promotes 6-TG-induced autophagy (A) Control luciferase (cont) or Chk1 siRNA were transfected into HCT116 (MLH1⁺, MMR⁺) cells, as described in the Materials and Methods. Chk1 protein levels were determined by immunoblot analysis with anti-Chk1. (B) HCT116 (MLH1⁺, MMR⁺) cells were treated with 3 μ mol/L 6-TG for 24h. Control luciferase (cont) or Chk1 siRNA oligos were then transfected to the cells as described above. At day 3 after exposure to 6-TG, the cells were harvested, stained with propidium iodide for cell cycle analysis (B) as described in the Materials and Methods or subjected to SDS-PAGE and immunoblot analysis with anti-LC3 (C). The amount of LC3-II and actin was quantified using NIH Image J and the ratio of LC3-II to actin was graphed in the lower panel,